

# Theoretical Study of Complexes of Extended Cyclopentadienyl Ligands with Zinc and Cadmium

Hong Seok Kang\*

College of Natural Science, Jeonju University, Hyoja-dong, Wansan-ku, Chonju, Chonbuk 560–759, Republic of Korea

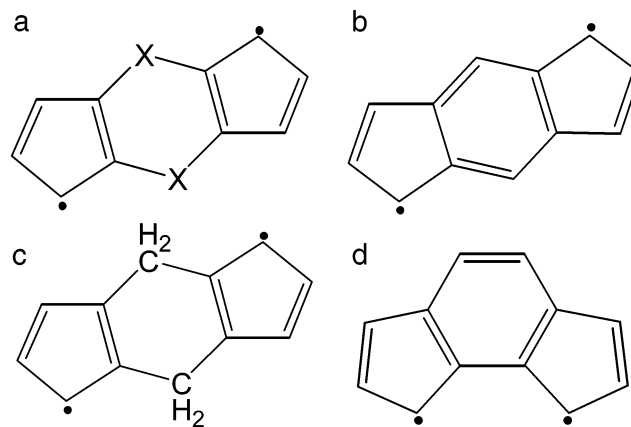
Received: December 15, 2004; In Final Form: February 1, 2005

Using density functional theory, we have theoretically studied various kinds of complexes of cyclopentadienyl and dicyclopentadienyl ligands with zinc and cadmium atoms of oxidation state +1. We first find that a sandwich complex  $\text{Cp}^*-\text{Zn}-\text{Zn}-\text{Cp}^*$  that was recently identified by Resta et al, (*Science* **2004**, 305, 1136) has a large overall binding energy ( $=-3.19$  eV), where  $\text{Cp}^*$  denotes the pentamethyl cyclopentadienyl group. In addition,  $\text{Cp}-\text{Zn}-\text{Zn}-\text{Cp}$  is found to have a binding energy even larger by 0.93 eV, where Cp is a cyclopentadienyl ligand without methyl groups attached. Electronic structure analysis shows accumulation of electron density between Zn atoms, confirming the existence of Zn–Zn bond that is as strong as typical transition metal-halide bonds. In addition, our calculation suggests the possible existence of similar complexes  $\text{Cp}^*-\text{Zn}-\text{Cd}-\text{Cp}^*$  and  $\text{Cp}-\text{Zn}-\text{Cd}-\text{Cp}$  with a Zn–Cd bond not known thus far. Furthermore, study on the dimetallic complexes of dicyclopentadienyl ligands also predicts results which hold potential application to organometallic chemistry and organic synthesis: (a) Complexes involving a stiff ligand Dp can presumably exist in the form of dimerized sandwich complexes  $\text{Dp}-2\text{M}_1-2\text{M}_2-\text{Dp}$  ( $\text{M}_1, \text{M}_2 = \text{Zn}, \text{Cd}$ ) with two metal–metal bonds. Their overall binding energies amount to  $-1.84$  to  $-3.48$  eV depending upon the kinds of metallic atoms, the strongest binding corresponding to dizinc complex. (b) Complexes involving more flexible ligand Ep can also form similar sandwich complexes  $\text{Ep}-2\text{M}_1-2\text{M}_2-\text{Ep}$ , but with much larger overall binding energies ( $=-4.97$  to  $-7.09$  eV). In addition, they can also exist in the form of nonsandwich complexes  $\text{M}_1-\text{Ep}-\text{M}_2$  involving only one ligand. Unlike most of dimetallic complexes of other transition metals, syn conformations are found to be exceptionally stable due to the formation of  $\text{M}_1-\text{M}_2$  bonds. Careful electronic structure analysis gives deep insight into the nature of observed phenomena.

## 1. Introduction

Very recently, X-ray structure determination has shown that zinc can exhibit the oxidation state of +1 with Zn–Zn bond in the sandwich complex of decamethylzincocene.<sup>1</sup> In view of the catalytic activity of transition metal complexes<sup>2</sup> as well as possible application of metallocene-containing dendrimers and polymers to nonlinear optics,<sup>3</sup> liquid crystals,<sup>4</sup> and sensors,<sup>5</sup> it can be potentially useful in wide range of areas from organic synthesis to molecular devices. Therefore, that finding will certainly stimulate synthesis and characterization of various kinds of organozinc complexes involving  $\text{Zn}_2^{2+}$  as final products as well as reaction intermediates. However, there is still no report for the direct evidence for the accumulation of electron density between two Zn atoms as a result of bonding interaction between atomic orbitals from the two atoms, requiring theoretical study on its electronic structure. Meanwhile, a question naturally arises if  $\text{Zn}^+-\text{Cd}^+$  with a Zn–Cd bond can also exist, noting that complexes involving  $\text{Cd}_2^{2+}$  with Cd–Cd bond are also known.<sup>6</sup> It is also possible that extended Cp sandwich systems with more than one Cp ring can have more than one Zn–Zn, Cd–Cd, or Zn–Cd bond in which Cp rings are connected by aromatic or alkyl chains (Scheme 1a), noting that stable forms of the Zn complex mostly involve aromatic cyclopentadienyl anion ( $\text{Cp}^{-1}$ ) with an excess electron transferred from Zn atoms. Since their chemical properties will be sensitively dependent upon the kind

**SCHEME 1: A General Drawing for a Ligand with Two Cyclopentadienyl Rings Connected by a Group of Atoms X (a), Neutral *s*-Indacenyl (Dp) (b), Ep (c), and *as*-Indacenyl Groups (d)**



of linking groups in the ligands, there can be big diversity in their organometallic chemistry. For this, we note that indenyl ligands (Scheme 1b) usually form dimetallic complexes,<sup>7,8</sup> while double silyl-bridging ( $\text{X} = \text{SiR}_2$  in Scheme 1a) of two Cp rings was known to form metallocene polymers.<sup>9</sup> In dimetallic complexes which do not form sandwich structures, conformation (syn or anti) of two metallic atoms with respect to the ligands as well as their binding strength will also depend on the kinds

\* E-mail: hsk@jj.ac.kr

**TABLE 1: Binding Energies in eV for the Processes P1, D1, and E1 Defined in the Table, Where Cp, Dp, and Ep Represent Neutral Cyclopentadienyl Group, Dicyclopentadienyl Group in Scheme 1b, and Dicyclopentadienyl Group in Scheme 1c, Respectively<sup>a</sup>**

process		$M_1 = \text{Zn}$		$M_1 = \text{Cd}$
		$M_2 = \text{Zn}$	$M_2 = \text{Cd}$	$M_2 = \text{Cd}$
P1 (P1*)	$\text{Cp}(\text{D}) + \text{M}_1 \rightarrow \text{Cp}-\text{M}_1(\text{D})$	-0.53 (-0.10)	-0.30 (-0.02)	
D1	$\text{Dp}(\text{S}) + \text{M}_1 + \text{M}_2 \rightarrow \text{M}_1-\text{Dp}-\text{M}_2(\text{S})$	-0.24	-0.08	-0.12
E1	$\text{Ep}(\text{T}) + \text{M}_1 + \text{M}_2 \rightarrow \text{M}_1-\text{Ep}-\text{M}_2(\text{S})$	-2.86	-2.37	-1.93

<sup>a</sup> In parentheses are also shown the binding energies for the process P1\* involving Cp\* instead of Cp. S, D, and T in parentheses denote that the spin multiplicity of the lowest energy structure for the corresponding compound is singlet, doublet, and triplet, respectively.

of ligands. In respect to general preference of anti conformation,<sup>7,8</sup> it is also of interest to investigate which conformations the extended Zn-Cp systems adopt in relation to their application to the selective synthesis of organometallic complexes in a controlled way. This work is motivated by all the questions addressed above, and we intend to find answers to at least some of them based on theoretical analysis.

## 2. Theoretical Methods

Our total energy calculations are performed using the Vienna ab initio simulation program (VASP).<sup>10,11</sup> Electron-ion interaction is described by the projector augmented wave (PAW) method,<sup>12</sup> which is basically a frozen-core all-electron calculation. Exchange-correlation effect was treated within the generalized gradient approximation due to Perdew, Burke, and Ernzerhof (PBE).<sup>13</sup> The solution of the Kohn-Sham (KS) equation was obtained using a Davison blocked iteration scheme followed by the residual vector minimization method.<sup>11</sup> All the valence electrons of chemical elements were explicitly considered in the KS equation. For zinc and cadmium, 10 3d and 4d electrons were also explicitly treated as valence electrons. We adopt a supercell geometry for which *k*-space sampling was done with  $\Gamma$ -point. For this, we use large supercells which guarantee interatomic distances between neighboring cells greater than 8.72 Å. Therefore, the size of the supercell depends on the size of the molecular system, the smallest one spanning (11, 11, and 16 Å) along three dimensions. Most of our results rely on the spin-polarized calculation. The cutoff energy is set high (=400 eV) enough to guarantee accurate results. The conjugate gradient method is employed to optimize the geometry until the Hellmann-Feynman force exerted on an atom is less than 0.03 eV/Å. Since our calculation relies on the plane wave basis, and not on the localized orbital basis, it should be noted that errors arising from the incompleteness of the basis set are systematically reduced as the cutoff energy is increased. For this, we note that our recent work on a benzene-Li-benzene sandwich complex showed that our PBE calculation using the same cutoff energy and the same convergence criterion was accurate within 0.1 eV when it was compared with the more sophisticated calculation G3(MP2).<sup>14</sup>

## 3. Results

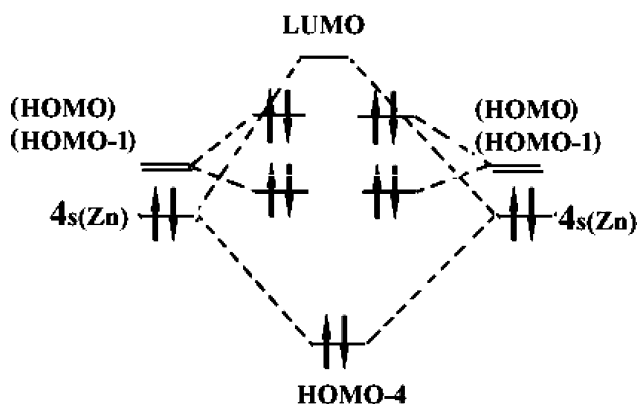
We first consider the system Cp-Zn-Zn-Cp, where Cp is a cyclopentadienyl group without a methyl group attached. We will also consider Resa et al's sandwich complex<sup>1</sup> Cp\*-Zn-Zn-Cp\* latter in this section, where Cp\* is a cyclopentadienyl ring functionalized with five methyl groups. Henceforth, the labels Cp and Cp\* are exclusively used to denote C<sub>5</sub>H<sub>5</sub> and C<sub>5</sub>(CH<sub>3</sub>)<sub>5</sub> groups, respectively. We describe the formation of Cp complex in two steps. The first step (P1) represents the formation of the complex Cp-M<sub>1</sub> from its neutral components, i.e., the process Cp+M<sub>1</sub> → Cp-M<sub>1</sub>. (See also Table 1.) The

**TABLE 2: Binding Energies ( $E_b$ ) of the Processes P2,  $\text{Cp}-\text{M}_1 + \text{Cp}-\text{M}_2 \rightarrow \text{Cp}-\text{M}_1-\text{M}_2-\text{Cp}$ , as Well as Those of the Overall Process  $2\text{P1} + \text{P2}$ , Where P1 Is Defined in Table 1<sup>a</sup>**

(M <sub>1</sub> ,M <sub>2</sub> )	(Zn, Zn)	(Cd, Cd)	(Zn, Cd)
$E_b(\text{P2})$	-3.06 (-2.99)	-2.34 (-1.88)	-2.69 (-2.41)
$E_b(2\text{P1} + \text{P2})$	-4.12 (-3.19)	-2.94 (-1.92)	-3.52 (-2.53)
$l(\text{M}_1-\text{M}_2)^b$	2.29 (2.28)	2.60 (2.60)	2.46 (2.45)
$o(\text{M}_1-\text{M}_2)^c$	0.87 (0.89)	0.86 (0.86)	0.86 (0.87)
$l(\text{M}-\text{Cp})^d$	1.98 (1.89)	2.21 (2.19)	1.98, 2.23 (1.91, 2.22)
$l(\text{M}-\text{C}_i^e)^e$	2.31 (2.28)	2.51 (2.53)	2.28, 2.53 (2.27, 2.54)
$q(\text{M})^f$	0.84 (0.86)	0.82 (0.83)	0.84, 0.84 (0.85, 0.84)

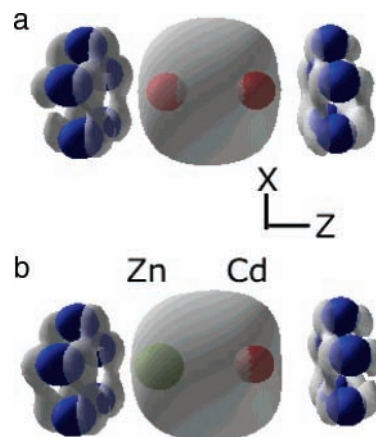
<sup>a</sup> Also shown are geometrical parameters of the products Cp-M<sub>1</sub>-M<sub>2</sub>-Cp, their Wiberg bond indices (WBI), and partial charges *q* on specified atoms of the complexes obtained from the natural bond order (NBO) analysis. Other parameters are explained in the footnotes. When two numbers appear in a line, they correspond to quantities involving M<sub>1</sub> and M<sub>2</sub> in order. In parentheses are also shown corresponding quantities for the process P2\* involving Cp\* instead of Cp. <sup>b</sup> Bond length of the bond M<sub>1</sub>-M<sub>2</sub>. <sup>c</sup> WBI for the bond M<sub>1</sub>-M<sub>2</sub>. <sup>d</sup> Distance from a metallic atom to the center of the adjacent Cp ring. <sup>e</sup> Interatomic distance between a metallic atom and a carbon atom in the adjacent Cp ring. Note that there are five equivalents. <sup>f</sup> NBO charge on metallic atoms. When two numbers appear, each of them corresponds to different M<sub>1</sub> and M<sub>2</sub>.

second step (P2) is concerned with dimer formation, i.e., the process Cp-M<sub>1</sub> + Cp-M<sub>2</sub> → Cp-M<sub>1</sub>-M<sub>2</sub>-Cp. Similar reactions involving other metallic atoms to be discussed latter will be also labeled this way. Our spin-polarized calculation shows that the complexes Cp-M<sub>1</sub>-M<sub>2</sub>-Cp are in the singlet states for all metals considered in this work. Table 2 shows that P2 is much more favorable than the process P1. The binding energy [ $E_b(\text{P2}) = -3.06$  eV] of the former process, which measures the strength of Zn-Zn binding, shows that it is larger than typical bond energies between transition metals and comparable to those for transition metal-halide bonds.<sup>15</sup> For comparison, we have also carried out structure optimization using PBEPBE exchange-correlational functional implemented in GAUSSIAN03 program<sup>16</sup> with a mixed basis set, i.e., a 6-31G(d) basis set for C and H and LanL2DZ set for Zn. (This basis set is used in all our GAUSSIAN calculations throughout this work.) We find that the binding energy (=−3.22 eV) for the process P2 is in good agreement with our result. When we consider the overall process 2Cp + 2Zn → Cp-2Zn-Cp, an even larger binding energy [ $E_b(2\text{P1} + \text{P2}) = -4.12$  eV in Table 2] from our calculation seems to be sufficient to expect the existence of the product unless it is chemically unstable. The optimized structure of Cp-2Zn-Cp is similar to the X-ray structure of Cp\*-2Zn-Cp\* other than the replacement of

**SCHEME 2: Simplified Energy Level Diagram of the Complex Cp–Zn–Zn–Cp<sup>a</sup>**


<sup>a</sup> Levels in parentheses denote those of Cp<sup>−</sup> anion.

methyl groups to hydrogen atoms.<sup>1</sup> There is a Zn–Zn bond which is oriented perpendicular to the planes of Cp with its bond length (=2.29 Å) close to the experimental value (=2.31 Å). The Zn–Cp distance (=1.98 Å) is also in reasonable agreement with the X-ray data (=2.04 Å). Analysis of the *l,m*-projected electronic local density of states (LDOS) at each atom and electron density maps for states around HOMO level shows that all the states derived from 3d-states of zinc atoms are located below HOMO-4, indicating relative inertness of d-electrons during the formation of this complex. Scheme 2 shows the energy level diagram. HOMO-4 is characterized by Zn–Zn  $\sigma$ -bond between two  $sp^{\delta}$  hybrid orbitals, where  $\delta$  is a small quantity. (See Figure 1a). This observation gives a very clear support for the existence of a direct Zn–Zn bond in this complex. The Wiberg bond index<sup>17</sup> (WBI) (=0.87) given in Table 2 also indicates that there is a single bond between them. HOMO-3 and HOMO-1 represent bonding and antibonding interactions between two (HOMO-1)  $\pi$  orbitals of two Cp<sup>−</sup> ions. (Henceforth, ligand orbitals are denoted by ligand levels in parentheses to distinguish them from those of a complex.) A small difference in the energy (=0.23 eV) between them indicates weakness of the  $\pi$ – $\pi$  interaction, as indicated by the large distance (=6.17 Å) between two Cp rings. Similarly, HOMO-2 and HOMO correspond to interactions of two (HOMO)s of Cp<sup>−</sup> ion. [In Scheme 2, (HOMO-1) and (HOMO) of the Cp<sup>−</sup> ring are not shown to be filled, since we are considering the process of forming the sandwich complex from neutral Cp rings and not from Cp<sup>−</sup> ion. However, we should note that there are total of six electrons coming from two Cp rings which occupy three Cp<sup>−</sup>-derived levels (possibly HOMO-3~HOMO-1) of the complex shown in the scheme.] In addition, HOMO-3 and HOMO-2 as well as HOMO-1 and HOMO are degenerate, which is originated from the degeneracy of (HOMO-1) and (HOMO) of Cp<sup>−</sup> ion. LUMO is derived from the antibonding interaction between two 4s(Zn) states. Upon the formation of Cp–Zn–Zn–Cp from their individual components, therefore, two of four 4s(Zn) electrons take part in the formation of a Zn–Zn  $\sigma$ -bond. The other two are transferred to HOMO of the complex to form Cp<sup>−</sup> anions, thus leaving the 4s(Zn)-derived LUMO state unoccupied. [If we imagine the situation where both of two 4s(Zn)-derived states are filled, we would not expect any significant charge transfer, leaving the Zn atom in the oxidation state of zero.] In short, Zn atoms are in the oxidation states of +1. In fact, Table 2 shows that our analysis of natural bond orbitals<sup>18</sup> (NBO) using GAUSSIAN03 program is consistent with this analysis, resulting in charges  $q = +0.84$  on Zn atoms. (This analysis was done by performing a single-

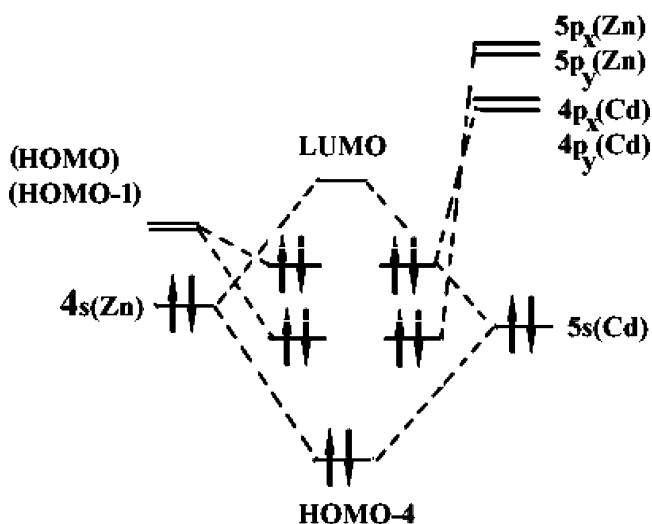


**Figure 1.** Electron density distributions in HOMO-4 for the complexes Cp–Zn–Zn–Cp (a) and Cp–Zn–Cd–Cp (b). For simplicity, hydrogen atoms are not shown. Metal–metal bond is directed along Z axis.

point GAUSSIAN calculation with the optimized geometry obtained from our VASP calculation.) This also shows that  $\eta^5$ -hapticity of Zn–Cp coordination is mostly related to the electrostatic interaction between Zn<sup>+</sup> and Cp<sup>−</sup> anion. Table 2 also shows some other useful parameters.

Next, we consider the complex Cp–Cd–Cd–Cp. Its optimized structure is very similar to that of its zinc analogue. As shown in Table 2, binding strength [ $E_b(P2) = -2.34$  eV] of the Cd–Cd bond, although weaker than the Zn–Zn bond described above, is comparable to those between other transition metals. In view of its still large binding energy [ $E_b(2P1 + P2) = -2.94$  eV in Table 2] for the overall process, it will be also interesting to see if the Cd-containing dimer can be also identified experimentally. Although not explicitly described here, its electronic structure is similar to that of its Zn analogue. Weaker binding in the Cd-complex compared to its Zn analogue seems to be partly related to the fact that 5s(Cd) state lies lower than the 4s(Zn) state by approximately 0.32 eV. If we consider transfer of two electrons from one of these states to HOMO of the complex upon the formation of Cp–Cd–Cd–Cp, we would expect that the gain in energy is less than that of its Zn correspondent by 0.64 eV, simply assuming that the energy levels of HOMOs are the same for both Zn- and Cd-containing complexes. In addition, Cd–Cd (=2.60 Å) and Cd–Cp (=2.21 Å) distances are longer than those for their Zn correspondents in Table 2. We also note that the former is consistent with that (=2.576 Å) found in the X-ray structure of Cd<sub>2</sub>(AlCl<sub>4</sub>)<sub>2</sub>.<sup>6</sup>

Now, we consider a hetero complex Cp–Zn–Cd–Cp. From Table 2, we first note that Cd–Zn binding [ $E_b(P2) = -2.69$  eV] is stronger than the Cd–Cd bond but weaker than the Zn–Zn bond. A similar argument holds for its overall binding energy [ $E_b(2P1 + P2) = -3.52$  eV]. It will be also interesting to see if this complex can be identified experimentally. When optimized, we find a structure similar to those of homocomplexes. Zn–Cd distance (=2.46 Å in Table 2) lies between Zn–Zn (=2.29 Å) and Cd–Cd (=2.60 Å) distances. Table 2 also shows that Zn–Cp (=1.98 Å) and Cd–Cp (2.23 Å) distances are similar to those in homocomplexes. Analysis of the electronic structure also gives us a clearer picture on the binding in the Cd-complexed dimer. States derived from d-states of both of Zn and Cd are again located below HOMO-4 of the complex. The energy level diagram is shown in Scheme 3. HOMO-4 is a bonding interaction between  $sp^{\delta}(\text{Zn})$  and  $sp^{\delta}(\text{Cd})$  orbitals. As in the case of homocomplexes, Figure 1b clearly shows large electron density between the two metal atoms in HOMO-4, strongly suggesting the existence of a Zn–Cd bond. As far as

**SCHEME 3: Simplified Energy Level Diagram of the Complex Cp–Zn–Cd–Cp<sup>a</sup>**

<sup>a</sup> Also see the caption for Scheme 2.

the author's knowledge is concerned, there has been no experimental report of the bond. The figure does not show any appreciable polarization of the electron density toward either of the two metallic atoms, which is consistent with the fact that there is no difference in the NBO charges ( $=0.84$ ) of the two metallic atoms in Table 2. HOMO-3 and HOMO-2, which are degenerate to each other, represent (HOMO-1) of a Cp<sup>-</sup> ring that is in symmetry-allowed interactions with p<sub>x</sub> and p<sub>y</sub> orbitals of the Zn atom, respectively. For this, we note that XY plane is parallel to the planes of the Cp<sup>-</sup> rings. (See Figure 1a for the definition of the coordinate system.) In contrast to the case of homodimetallic complexes, electron density is concentrated on only Zn atom and a Cp<sup>-</sup> ring nearby, being negligible around both the Cd atom and the other Cp<sup>-</sup> ring [=Cp<sup>-</sup>(Cd)]. Similarly, HOMO-1 and HOMO are characterized by (HOMO-1) of the Cp<sup>-</sup>(Cd) in similar interactions with p<sub>x</sub> and p<sub>y</sub> orbitals of the Cd atom, respectively. Again, electron density is negligible around the Zn atom and Cp<sup>-</sup>(Zn). Similar to the case of the homocomplexes, LUMO represents the antibonding interaction between 4s(Zn) and 5s(Cd) orbitals, again confirming the charge transfer to HOMO of the complex.

We next consider the system Cp<sup>\*-</sup>Zn–Zn–Cp<sup>\*-</sup>. Comparison of its binding energy with that of its Cp-correspondent will give us information on the role of methyl groups in energetics of the system. Table 1 shows that there is practically no binding in the process P1\*, Cp<sup>\*-</sup> + M<sub>1</sub> → Cp<sup>\*-</sup>–M<sub>1</sub>. [We denote processes similar to P1 and P2 involving Cp<sup>\*</sup> (instead of Cp) by P1\* and P2\*.] Although the binding strength ( $=-2.99$  eV) of the Zn–Zn bond is almost the same as in the complex involving Cp, the overall binding energy [ $E_b(2P1^* + P2^*) = -3.19$  eV in Table 2] of the complex is 0.93 eV smaller. The reason for this can be also understood from the electronic structure analysis. We find that HOMO-4~HOMO of the complex can be depicted by a scheme similar to that shown in Scheme 2.<sup>19</sup> In a simple model, therefore, we can expect that two 4s(Zn) electrons are transferred to HOMO of the complex upon the its formation from their individual components. This also implies that the observed overall binding energy, which is smaller than that for its Cp analogue by 0.93 eV, is due to the destabilization of HOMO of the Cp<sup>\*</sup> complex. In fact, we find that the all the levels HOMO-3~HOMO are shifted toward higher energy by the same amount. Specifically, the HOMO-4–HOMO gap of the dimer is 0.52 eV larger than that of Cp–

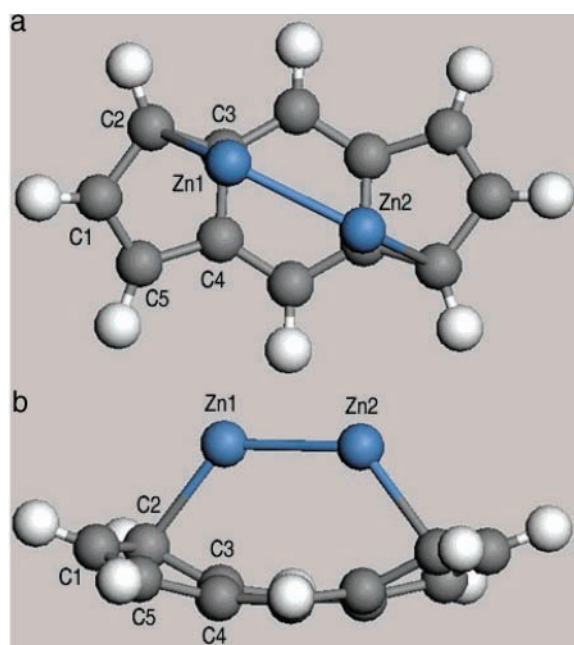
Zn–Zn–Cp. For this, we note that HOMO-4 of the Cp<sup>\*</sup> complex also represents the 4s(Zn)–4s(Zn) bonding, and its energy level would not be largely different from that of its Cp analogue, Cp–Zn–Zn–Cp. This is because its electron density is concentrated on the region between two Zn atoms which are approximately 3.39 Å apart from methyl groups. On the other hand, energy level of HOMO of the complex, which is an antibonding interaction between π orbitals of the Cp<sup>\*-</sup> anions, should be more affected by the presence of 10 methyl groups in Cp<sup>\*</sup> rings. This is because the groups effectively constitute a box which confines the π orbitals in smaller space, destabilizing them. Since two electrons are involved in the transfer to this HOMO, we can expect that the overall binding energy of the Cp<sup>\*</sup> complex would be roughly 1.04 eV smaller than that of its Cp analogue, accounting for the observed difference in energy ( $=0.93$  eV). Very weak binding for the process P1\* [ $E_b(P1^*) = -0.10$  eV in Table 1] can be similarly explained. Table 2 shows that geometrical parameters, NBO charges, and bond orders of various components of the complex are similar to those in its Cp analogue. Considering that the Cp<sup>\*</sup> complex do exist and its Cp analogue is energetically even more stable, we can easily expect that the Cp complex would be able to be identified experimentally, unless it is easily subject to other kinds of chemical reactions.

Now we consider the complex involving *s*-indacenyl dianion (Dp<sup>-2</sup>), two five-membered cyclopentadienyl anion rings fused into a central benzene ring. [See Scheme 1b for its neutral correspondent.] For simplicity, we consider the Dp ring without methyl groups attached. Again, we consider two steps for possible formation of the complex Dp–2Zn–2Zn–Dp. The first step (D1) is the formation of the complex Dp–2Zn, while the second one (D2) represents its dimer formation through possible creation of two stable Zn–Zn bonds. In process D1, we find that the syn conformation (S) in which two Zn atoms are located on the same side of the Dp ring is slightly more stable (by 0.17 eV) than the anti conformation (S) with them on the opposite sides. Spin multiplicities in parentheses indicate that our VASP calculation shows that both of them are in singlet ground states. In the optimized structure (C<sub>2</sub> symmetry in Table 3) of the syn complex shown in Figure 2, we find a weak Zn–Zn bond with the bond length ( $=2.51$  Å) about 10% longer than that ( $=2.29$  Å) in the complex Cp–Zn–Zn–Cp discussed above. For comparison, we note that this preference, although small, is different from our previous calculation on the naphthalene–2Li complex<sup>14</sup> (S) which showed that it preferred the anti conformation (S) by 0.15 eV. Considering that there is also a large charge transfer from the Li atoms to the naphthalene ring in that case, at a glance, adoption of anti conformation is expected to be more favorable due to the reduction of electrostatic repulsion between positively charged Li ions. Our contradictory observation suggests that energy gain resulting from the formation of the weak Zn–Zn bond in Dp–2Zn does more than compensating for the energy loss due to the electrostatic repulsion between partially charged Zn atoms in the syn conformation. In fact, our separate electronic structure analysis shows that about 50% of the electron density of HOMO-3 of this complex represents a σ bond between 4s(Zn) states, while the other 50% represents a π state of the Dp<sup>-2</sup> ring. Wiberg bond index ( $=0.48$  in Table 3) for the Zn–Zn bond is consistent with this observation. Complete filling up to (HOMO) of Dp<sup>-2</sup> also implies appreciable charge transfer from Zn atoms to the Dp ring, which is also consistent with the NBO charge ( $=0.63$  in Table 3) of Zn atoms. Most of Zn–C<sub>i</sub><sup>5</sup> distances in Table 3 are longer than those ( $=2.31$  Å in Table

**TABLE 3: Binding Energies ( $E_b$ ) for the Processes D1 and E1 Defined in Table 1<sup>a</sup>**

	Zn–Dp–Zn	Cd–Dp–Cd	Zn–Dp–Cd	Zn–Ep–Zn	Cd–Ep–Cd	Zn–Ep–Cd
(M <sub>1</sub> , M <sub>2</sub> )	(Zn, Zn)	(Cd, Cd)	(Zn, Cd)	(Zn, Zn)	(Cd, Cd)	(Zn, Cd)
point group	$C_2$	$C_2$	$C_s$	$C_{2v}$	$C_{2v}$	$C_s$
process	D1	D1	D1	E1	E1	E1
conformation	syn	syn	syn	syn	syn	syn
multiplicity	singlet	singlet	singlet	singlet	singlet	singlet
$E_b$ (eV) <sup>b</sup>	−0.24	−0.12	−0.08	−2.86	−1.93	−2.37
$l$ (M <sub>1</sub> –M <sub>2</sub> ) <sup>c</sup>	2.51	3.50	3.32	2.33	2.68	2.51
$O$ (M <sub>1</sub> –M <sub>2</sub> ) <sup>d</sup>	0.48	0.05	0.05	0.73	0.57	0.66
$l$ (M–C <sub>1</sub> <sup>5</sup> ) <sup>e</sup>	2.80	4.12	4.11, 4.06	2.14	2.36	2.12, 2.38
	2.23	3.82	3.90, 3.88	2.34	2.64	2.36, 2.61
	2.41	3.72	3.73, 3.75	2.60	2.99	2.67, 2.89
	2.83	3.95	3.73, 3.75	2.60	2.99	2.67, 2.89
	3.12	4.19	3.90, 3.88	2.34	2.64	2.36, 2.61
$q$ (M) <sup>f</sup>	0.63	0.01	−0.01, −0.01	0.78	0.67	0.75, 0.71
$l$ (C <sub>1</sub> <sup>5</sup> –C <sub>1+1</sub> <sup>5</sup> ) <sup>g</sup>	1.46	1.41	1.41, 1.41	1.45	1.45	1.45, 1.45
	1.46	1.42	1.43, 1.43	1.41	1.40	1.41, 1.41
	1.45	1.45	1.45, 1.45	1.43	1.44	1.43, 1.43
	1.44	1.42	1.43, 1.43	1.41	1.40	1.41, 1.41
	1.38	1.41	1.41, 1.41	1.45	1.45	1.45, 1.45

<sup>a</sup> Also shown are geometrical parameters of the products, their Wiberg bond indices (WBI), and partial charges  $q$  on specified atoms of the complexes obtained from the natural bond order (NBO) analysis. Other parameters are explained in the footnotes. When two numbers appear, they correspond to quantities involving M<sub>1</sub> and M<sub>2</sub> in order. <sup>b</sup> Binding energy of the corresponding process. <sup>c</sup> Bond length between two metallic atoms. <sup>d</sup> WBI for the bond between two metallic atoms. <sup>e</sup> Interatomic distances between a metallic atom and a carbon atom in the adjacent five-membered ring. See Figure 2a for the convention of labeling. <sup>f</sup> NBO charge on metallic atoms. <sup>g</sup> Bond lengths between (C<sub>1</sub>,C<sub>2</sub>), (C<sub>2</sub>,C<sub>3</sub>), (C<sub>3</sub>,C<sub>4</sub>), (C<sub>4</sub>,C<sub>5</sub>), and (C<sub>5</sub>,C<sub>1</sub>). Also see footnote *e* above.

**Figure 2.** Optimized structure of Zn–Dp–Zn viewed along two axes.

2) in Cp–Zn–Zn–Cp, where C<sub>*i*</sub><sup>5</sup> denotes an atom in a five-membered cyclopentadienyl ring. See Figure 2a for the way they are labeled. [Superscript 5 is sometimes used to emphasize that the atom belongs to a five-membered ring.] Two five-membered rings are bent to form an arc. [See Figure 2b.] It is worth noting that a similar bending was observed for the doubly silyl-bridged ligand in the X-ray structure of chromocenes.<sup>20</sup> Noting that C<sub>*i*</sub><sup>5</sup>–C<sub>*i*+1</sub><sup>5</sup> bond distances of a neutral Dp ring are 1.41, 1.43, 1.45, 1.43, and 1.41 Å for C<sub>1</sub><sup>5</sup>–C<sub>2</sub><sup>5</sup>, C<sub>2</sub><sup>5</sup>–C<sub>3</sub><sup>5</sup>, C<sub>3</sub><sup>5</sup>–C<sub>4</sub><sup>5</sup>, C<sub>4</sub><sup>5</sup>–C<sub>5</sub><sup>5</sup>, and C<sub>4</sub><sup>5</sup>–C<sub>5</sub><sup>1</sup> bonds, we find that the first two bonds are elongated and the last one is shortened. In fact, the complicated hapticity which deviates from ideal η<sup>5</sup> is related to the formation of weak covalent bonds between Zn and C<sub>*i*</sub><sup>5</sup>.<sup>21</sup>

Table 4 shows that dimer formation [ $E_b$ (D2) = −3.00 eV] is as much favorable as the corresponding process, P2, for the

complex Cp–Zn–Zn–Cp. Although overall binding energy [ $E_b$ –(2D1 + D2) = −3.48 eV] is smaller, it still suggests the possible existence of the dimer Dp–2Zn–2Zn–Dp. In short, we can expect that complexes of Dp and Zn could mostly exist in the form of the dimer rather than as monomers Dp–2Zn. Figure 3 shows its optimized structure ( $C_{2h}$ ). We note that Zn–Zn bond is not perpendicular to the ring planes. In fact, our constrained optimization in which the perpendicularity is compelled shows that such a conformation is less stable by 0.20 eV. Upon reoptimization after removal of the constraint, we again get the  $C_{2h}$  structure. This indirectly shows that our structure optimization can indeed bring the system of concern to the correct structure. Table 4 also shows various geometrical parameters, WBI, and NBO charges of its components.<sup>22</sup> Importantly, there are two Zn–Zn bonds with bond lengths (=2.32 Å in Table 4) close to that (=2.29 Å) in the complex Cp–2Zn–Cp. A simplified energy level diagram is shown in Scheme 4 for better understanding. First of all, HOMO–6 largely represents Zn–Zn single bonds through the overlap of 4s(Zn) orbitals, also confirming the existence of two Zn–Zn bonds. (Also see Figure 4.) Six states from HOMO–5 to HOMO are basically interactions between bonding π states of two Dp<sup>−2</sup> rings. Again, filling of all the dianion-derived states up to (HOMO) indeed signifies dianion formation through transfer of four electrons from four Zn atoms. LUMO is characterized by bonding interactions of p<sub>*x*</sub>(Zn1)–p<sub>*x*</sub>(Zn2) and p<sub>*x*</sub>(Zn3)–p<sub>*x*</sub>(Zn4), where the lobes of p<sub>*x*</sub>(Zn) are oriented normal to the Zn–Zn bonds.<sup>23</sup>

Next, we consider two steps for possible formation of the complex Dp–2Cd–2Cd–Dp. Optimized structure of Dp–2Cd is similar to that of Dp–2Zn. However, its binding is weaker, and this is manifested in all the parameters in Table 3.<sup>24</sup> We list only a few of them here. The Cd–Cd distance (=3.50 Å in Table 3) is 36% larger than that in Cp–Cd–Cd–Cp. WBI indicates that there is practically no Cd–Cd bond. In addition, there is little charge transfer from Cd atoms to the Dp rings, as evidenced by a very small NBO charge (=0.01 in Table 3) on Cd atoms. Table 4 shows that the binding energies of the dimerization processes D2 and the overall process 2D1 + D2

**TABLE 4: Binding Energies ( $E_b$ ) for the Processes (D2) of Dimer Formation<sup>a</sup>**

(M <sub>1</sub> , M <sub>2</sub> )	(Zn, Zn)	(Cd, Cd)	(Zn, Cd)		
			isomer 1	isomer 2	isomer 3
point group	$C_{2h}$	$C_{2h}$	$C_s$	$C_i$	$C_2$
$E_b(D2)$	-3.00	-1.60	-2.27	-2.27	-2.46
$E_b(2D1 + D2)$	-3.48	-1.84	-2.63	-2.43	-2.62
$l(M_1-M_2)$	2.32	2.68	2.50	2.50	2.34, 2.67
$l(M-C_i^5)$	2.34	2.72	2.41, 2.72	2.31, 2.73	2.38, 2.69
	2.06	2.26	2.05, 2.25	2.08, 2.26	2.05, 2.26
	2.52	2.80	2.56, 2.78	2.51, 2.80	2.55, 2.80
	2.89	3.34	3.00, 3.33	2.85, 3.33	2.97, 3.31
	2.78	3.29	2.90, 3.28	2.72, 3.28	2.87, 3.24
$l(C_i^5-C_{i+1}^5)$	1.46	1.47	1.46, 1.47	1.46, 1.47	1.46, 1.47
	1.46	1.47	1.47, 1.47	1.46, 1.47	1.47, 1.47
	1.45	1.45	1.45, 1.45	1.45, 1.45	1.45, 1.45
	1.44	1.44	1.44, 1.44	1.44, 1.44	1.44, 1.44
	1.39	1.38	1.39, 1.38	1.40, 1.38	1.39, 1.38
$q(C_i^5)$	-0.38	-0.33	-0.35, -0.33	-0.40, -0.32	-0.37, -0.34
	-0.65	-0.63	-0.66, -0.64	-0.62, -0.65	-0.66, -0.63
	-0.13	-0.11	-0.12, -0.11	-0.14, -0.10	-0.13, -0.11
	-0.11	-0.10	-0.11, -0.10	-0.12, -0.10	-0.11, -0.10
	-0.33	-0.29	-0.31, -0.29	-0.34, -0.30	-0.32, -0.30
$q(M)$	0.77	0.69	0.73, 0.75	0.74, 0.75	0.78, 0.69
$O(M_1-M_2)$	0.72	0.58	0.65	0.67	0.72, 0.58

<sup>a</sup>For (M<sub>1</sub>, M<sub>2</sub>) = (Zn, Zn) and (Cd, Cd), they correspond to the processes  $2M_1-Dp + 2M_2-Dp \rightarrow Dp-2M_1-2M_2-Dp$ . For (M<sub>1</sub>, M<sub>2</sub>) = (Zn, Cd), three isomers are described. Isomer 1 denotes the product of the process  $Zn-Dp-Zn + Cd-Dp-Cd \rightarrow Dp-2Zn-2Cd-Dp$ . On one hand, isomers 2 and 3 are obtained from the processes  $Zn-Dp-Cd + Zn-Dp-Cd \rightarrow Dp-2Zn-2Cd-Dp$ . The former forms two Zn-Cd bonds, while the latter forms one Zn-Zn and one Cd-Cd bond. Also shown are binding energies of the overall processes  $2D1 + D2$ , where D1 is defined in Table 1. Furthermore, geometrical and some other parameters of the products are also shown. Wiberg bond indices (WBI) and partial charges  $q$  on specified atoms of the complexes were obtained from the natural bond order (NBO) analysis from the GAUSSIAN03 calculations. When two numbers appear, they correspond to quantities involving M<sub>1</sub> and M<sub>2</sub> in their orders. Also see footnotes of Table 3 for more details.

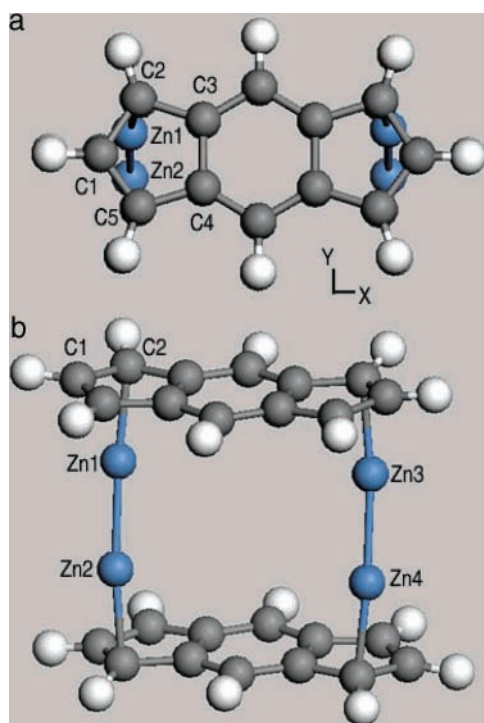
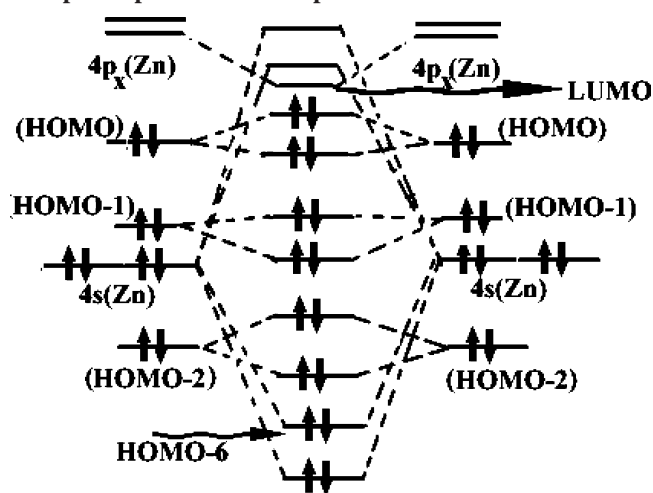


**Figure 3.** Optimized structure of  $Dp-2Zn-2Zn-Dp$  viewed along Z (a) and Y (b) axes. The latter one was slightly rotated along X axis for better understanding.

are about half of those of the corresponding process involving 4Zn atoms, suggesting that the stability of  $Dp-2Cd-2Cd-Dp$  is less pronounced. This is manifested in the smaller NBO charge ( $=0.69$ ) of Cd atoms and smaller WBI ( $=0.58$ ) of Cd-Cd bonds. Its optimized structure is similar to that for  $Dp-2Zn-2Zn-Dp$  shown in Figure 3.

Complex formation of Dp with both of Zn and Cd would be also interesting. For this, we first consider the formation of Zn-

**SCHEME 4: Simplified Energy Level Diagram of the Complex  $Dp-2Zn-2Zn-Dp$ <sup>a</sup>**



<sup>a</sup> Also see the caption for Scheme 2.

$Dp-Cd$ , corresponding to the process D1 in Table 1. Tables 1 and 3 show that the binding of the complex is also weak [ $E_b(D1) = -0.08$  eV], as is also manifested in other parameters in Table 3. As shown in Figure 5, its optimized structure exhibits symmetry ( $C_s$  in Table 3) different from that for homocomplexes. Again, we consider the dimerization process which produces the complex  $Dp-2Zn-2Cd-Dp$ , for which there are three possible isomers of nearly the same binding energy as indicated in Table 4. Isomer 1 is defined by the process  $D2$ ,  $Dp-2Zn + Dp-2Cd \rightarrow Dp-2Zn-2Cd-Dp$ , forming two Zn-Cd bonds. Its optimized structure is similar to that for  $Dp-2Zn-2Zn-Dp$  shown in Figure 3, if we substitute Zn2 and Zn4 with Cd atoms. Table 4 shows various parameters. Binding energy data show that the complex formation is more favorable than that of the homocomplexes involving Cd atoms only, but

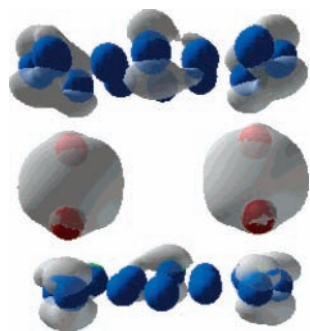


**Figure 4.** Electron density distribution in HOMO-6 for the complex Dp-2Zn-2Zn-Dp corresponding to Figure 3b. For simplicity, hydrogen atoms are not shown.

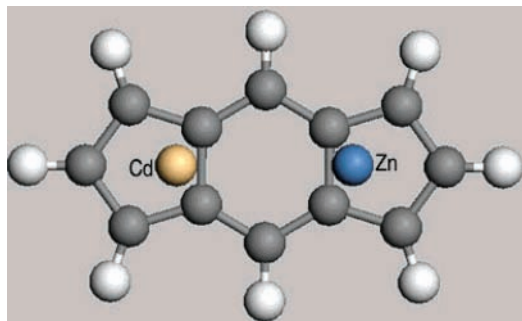


**Figure 5.** Optimized structure of Zn-Dp-Cd.

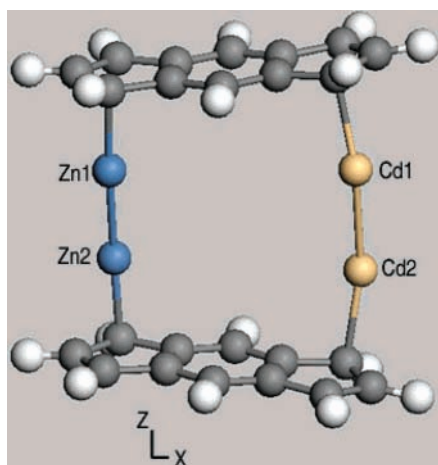


**Figure 6.** Optimized structure of isomer 3 of Dp-2Zn-2Cd-Dp viewed along the direction which is the same as in Figure 3b.

less favorable than the correspondent involving Zn atoms only. Other parameters in the table show no peculiarity in view of those of homocomplexes. Isomers **2** and **3** are formed in the process  $\text{Zn-Dp-Cd} + \text{Zn-Dp-Cd} \rightarrow \text{Dp-2Zn-2Cd-Dp}$ . They are distinguished from each other by the way metal-metal bonds are formed. In isomer **2**, a pair of Zn-Cd bonds are formed, while a Zn-Zn bond as well as a Cd-Cd bond is formed in isomer **3**. The optimized structure of isomer **2** is again similar to that for Dp-2Zn-2Zn-Dp, if we substitute Zn2 and Zn3 by Cd atoms. Its parameters in Table 4 are similar to those for the isomer **1**. Isomer **3**, whose optimized structure is shown in Figure 6, also shows no peculiarity in its parameters. In all the three isomers, Zn-Cd bonds are nonpolar.<sup>25</sup>

Scheme 1c shows another neutral dicyclopentadienyl derivative Ep in which two five-membered rings are bridged by two CH<sub>2</sub> groups. For simplicity, we also consider the case when there is no functional group attached to the rings. We first find

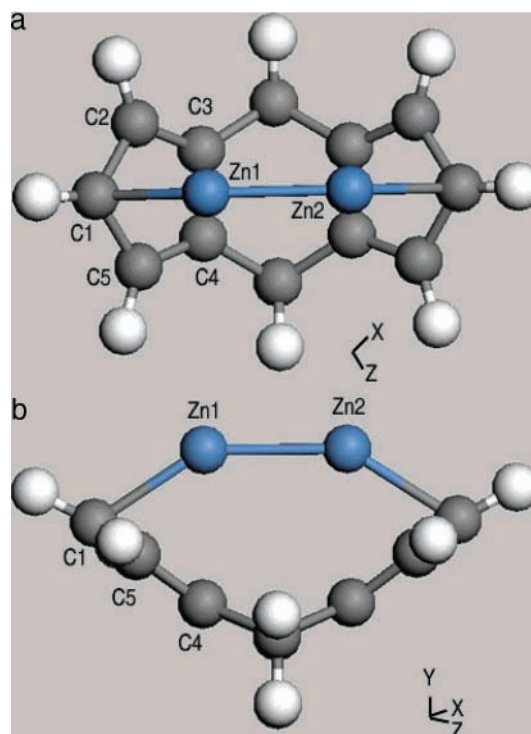


**Figure 7.** Optimized structure of Zn-Ep-Zn viewed along two directions defined in the coordinate system.

that the neutral Ep is in the triplet ground state that is more stable than the singlet state by approximately 0.42 eV. This is different from the case of Dp and implies that two cyclopentadienyl rings do not make appreciable interaction with each other through CH<sub>2</sub> groups. When we consider the process  $\text{Ep(T)} + 2\text{Zn(S)} \rightarrow \text{Ep-2Zn(S)}$ , Table 1 shows that its binding energy is -2.86 eV. Its product ( $C_{2v}$  symmetry as shown in Table 3) adopts syn conformation with respect to two Zn atoms. The anti conformation (T) with triplet ground state is found to be much less stable (by 2.21 eV). Observed large binding energy is in striking contrast to that [ $E_b(\text{D1}) = -0.24$  eV in Tables 1 and 3] of Dp-2Zn. This is also in contrast with the general preference of anti conformation reported for Dp.<sup>8</sup> It has been known that the anti preference is even stronger in the transition metal complexes involving an isomer of Dp shown in Scheme 1d.<sup>7</sup> Noting that the syn complex of Dp with rhodium is formed only under the specific condition which prevents the formation of the anti conformation,<sup>8</sup> the physically stable syn complex Ep-2Zn, unless it is easily subject to other chemical reactions, may hold potential application to organometallic chemistry. Then, the natural question is where the large binding energy of the monomer Ep-2Zn originated from. Figure 7 suggests that it is primarily due to the formation of a stable Zn-Zn bond. In the case of Dp complexes with Zn, we recall that the Zn-Zn bond was found to be energetically favorable only in the dimer Dp-2Zn-2Zn-Dp, not in the monomer Dp-2Zn. Table 3 indeed shows that the Zn-Zn distance ( $=2.33$  Å) in the optimized structure of Ep-2Zn is very close to those ( $=2.29$  and  $2.32$  Å) in those dimers, Cp-Zn-Zn-Cp and Dp-2Zn-2Zn-Dp. In addition, bond order ( $=0.73$ ) between Zn atoms shown in Table 3 also supports the single bond formation between the two Zn atoms. Table 3 also shows that Zn-C<sub>i</sub><sup>5</sup> distances are comparable to those in Dp-Zn2-Zn2-Dp in Table 4, also implying that the Zn-ring interaction can be described by distorted  $\eta^5$  hapticity.<sup>26</sup> The C<sub>1</sub><sup>5</sup> atom, an atom in the five-membered ring which is the closest to the Ep ring, accommodates around itself much of the excess electron density

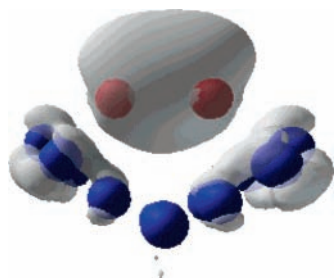


**Figure 8.** Electron density distribution in HOMO-4 of the complex Zn-Ep-Zn viewed along the same direction as in Figure 7b. For simplicity, hydrogen atoms are not shown.

( $q = -0.57$ ) transferred from the Zn atom nearby. Figure 7b shows that the six-membered ring is folded along the central CH<sub>2</sub> groups, which should facilitate complexation with  $\eta^5$  hapticity. The folding is more pronounced than the case of its Dp analogue shown in Figure 2b. Deformation is concentrated on the central six-membered ring, not on the two cyclopentadienyl rings. Again, electronic structure analysis gives us a clearer picture. As shown in Figure 8, HOMO-4 corresponds to a Zn-Zn  $\sigma$  bond originated from the interaction of 4s(Zn) states. HOMO-3~HOMO are mostly Ep<sup>-2</sup> ring states, in which distorted  $\eta^5$  hapticity of Zn-(five membered ring) interaction is manifested.<sup>27</sup> A large portion of LUMO represents antibonding interaction between 4s(Zn) states, again indicating transfer of two electrons from Zn atoms to ring states in consistency with the NBO analysis. (See Table 3.) If we imagine the situation where all the 4s(Zn)-derived states are filled, we would not expect any significant charge transfer.

Table 5 shows various parameters related to the dimerization process (E2), Ep-2Zn + Ep-2Zn  $\rightarrow$  Ep-2Zn-2Zn-Ep. Figure 9 shows the optimized structure ( $=D_{2h}$  symmetry as shown in Table 5) of the dimer, which is different from that for its Dp analogue. The  $D_{2h}$  symmetry was again confirmed by another optimization starting from an initial structure ( $C_{2h}$ )

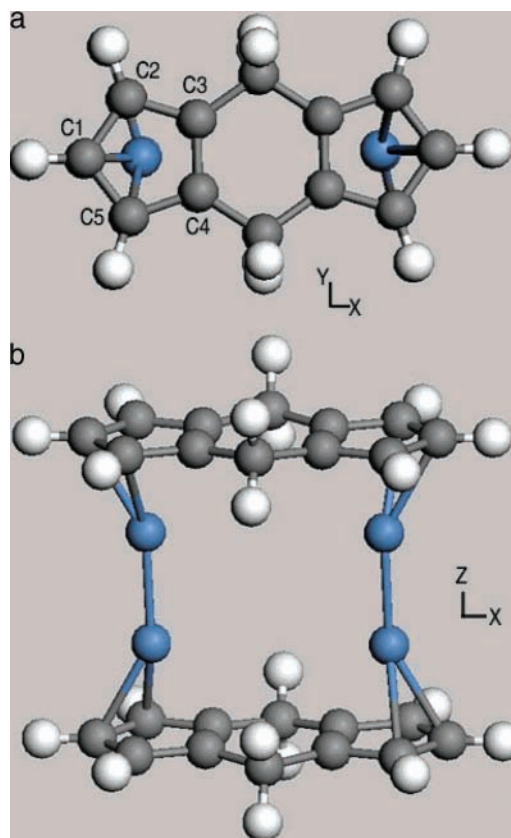


**Figure 9.** Optimized structure of Ep-2Zn-2Zn-Ep viewed along Z (a) and Y (b) axes. The latter one was slightly rotated along X axis for better understanding.

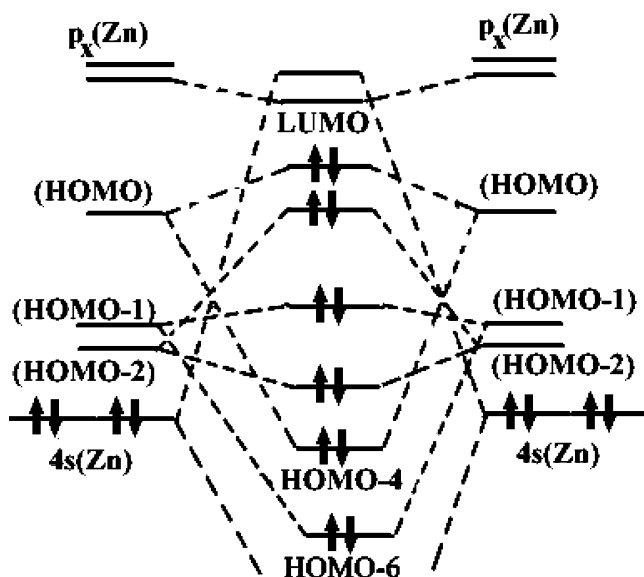
which is similar to that shown in Figure 3. From the fact that the binding energy [ $E_b(E2) = -1.66$  eV in Table 5] of the individual Zn-Zn bond is about half of that [ $E_b(D2) = -3.00$  eV in Table 4] in its Dp analogue, we find that the Zn-Ep

**TABLE 5: Binding Energies ( $E_b$ ) for the Processes (E2) of Dimer Formation<sup>a</sup>**

(M <sub>1</sub> , M <sub>2</sub> )			(Zn, Cd)		
	(Zn, Zn)	(Cd, Cd)	isomer 1	isomer 2	isomer 3
point group	$D_{2h}$	$D_{2h}$	$C_s$	$C_{2h}$	$C_{2v}$
$E_b(E2)$	-1.66	-1.11	-1.36	-1.45	-1.45
$E_b(2E1 + E2)$	-7.09	-4.97	-6.16	-6.19	-6.19
$l(M_1-M_2)$	2.29	2.60	2.43	2.44	2.30, 2.60
$l(M-C_i^5)$	2.24	2.41	2.25, 2.50	2.27, 2.43	2.27, 2.40
	2.26	2.50	2.25, 2.48	2.28, 2.55	2.28, 2.50
	2.34	2.66	2.31, 2.55	2.33, 2.68	2.33, 2.67
	2.34	2.66	2.31, 2.55	2.33, 2.68	2.33, 2.67
	2.26	2.50	2.25, 2.48	2.28, 2.55	2.28, 2.50
$l(C_i^5 - C_{i+1}^5)$	1.43	1.43	1.43, 1.43	1.43, 1.43	1.43, 1.43
	1.43	1.43	1.43, 1.43	1.43, 1.43	1.43, 1.43
	1.43	1.43	1.43, 1.43	1.44, 1.43	1.43, 1.43
	1.43	1.43	1.43, 1.43	1.43, 1.43	1.43, 1.42
	1.43	1.43	1.43, 1.43	1.43, 1.43	1.43, 1.43
$q(C_i)$	-0.44	-0.45	-0.44, -0.42	-0.43, -0.45	-0.43, -0.45
	-0.43	-0.44	-0.43, -0.38	-0.44, -0.43	-0.40, -0.43
	-0.18	-0.16	-0.19, -0.15	-0.23, -0.16	-0.15, -0.19
	-0.18	-0.16	-0.19, -0.19	-0.23, -0.16	-0.15, -0.19
	-0.43	-0.44	-0.44, -0.46	-0.44, -0.43	-0.40, -0.43
$q(M)$	0.85	0.81	0.83, 0.83	0.85, 0.82	0.85, 0.83
$O(M_1-M_2)$	0.88	0.84	0.85	0.86	0.88, 0.83

<sup>a</sup> For (M<sub>1</sub>, M<sub>2</sub>) = (Zn, Zn) and (Cd, Cd), they correspond to the process 2M<sub>1</sub>-Ep + 2M<sub>2</sub>-Ep  $\rightarrow$  Ep-2M<sub>1</sub>-M<sub>2</sub>-Ep. For (M<sub>1</sub>, M<sub>2</sub>) = (Zn, Cd), three isomers are described. Each isomer is defined in a way similar to that in Table 4. Also shown are binding energies for the overall processes 2E1 + E2, where E1 is defined in Table 1. Furthermore, geometrical and some other parameters of the products are also shown. Wiberg bond indices (WBI) and partial charges  $q$  on specified atoms of the complexes were obtained from the natural bond order (NBO) analysis from the GAUSSIAN03 calculations. When two numbers appear, they correspond to quantities involving M<sub>1</sub> and M<sub>2</sub> in their orders. Also see footnotes of Table 3 for more details.



**SCHEME 5: Simplified Energy Level Diagram of the Complex  $\text{Ep}-2\text{Zn}-2\text{Zn}-\text{Ep}^a$** 

<sup>a</sup> HOMO-5 of the complex is not shown. Also see the caption for Scheme 2

complex can exist as both monomers and dimers. (On the other hand, the Zn-Dp complex can only exist as dimers.) The table shows that Zn-Zn distance ( $=2.29 \text{ \AA}$ ) is the same as that in the Cp-Zn-Zn-Cp.  $\text{C}_1^5$  is the closest to a Zn atom. Excess electron density is also shown to be concentrated on three carbon atoms around it, as indicated by the NBO charges on five  $\text{C}_i^5$  atoms. Charges ( $=0.85$ ) on Zn atoms as well as Zn-Zn bond order ( $=0.88$ ) are almost the same as those in Cp-Zn-Zn-Cp.  $\text{C}_i-\text{C}_{i+1}$  distances are the same as those ( $=1.43 \text{ \AA}$ ) in an isolated dianion  $\text{Ep}^{2-}$ . Scheme 5 shows the energy level diagram of the dimer. We first note that dianion states are filled up to (HOMO), again confirming the transfer of approximately four electrons from four Zn atoms to form two dianions. To describe the electronic structure in more detail, HOMO-4 and HOMO represent the interactions of two (HOMO)s of two dianions, HOMO-3 and HOMO-1, those of (HOMO-2), and HOMO-6 and HOMO-2, those of (HOMO-1). LUMO is simply a bonding interaction between  $p_x(\text{Zn})$  orbitals.

Here, we consider similar complexes involving Cd instead of Zn. When we consider the process E1,  $\text{Ep}(\text{T}) + 2\text{Cd}(\text{S}) \rightarrow \text{Ep}-2\text{Cd}(\text{S})$ , of forming  $\text{Ep}-2\text{Cd}$  complex, we also find that the syn complex (S) is more stable than the anti complex (T) in triplet ground state. Its preference ( $=0.57 \text{ eV}$ ) is less pronounced than in the case of its Zn analogue. For the syn product, Table 3 shows that the binding energy [ $E_b(\text{E1}) = -1.93 \text{ eV}$ ] is also much larger than that [ $E_b(\text{D1}) = -0.12 \text{ eV}$ ] for the process forming Dp-2Cd, also strongly suggesting its possible existence through the formation of a Cd-Cd bond. In fact, Cd-Cd distance ( $=2.68 \text{ \AA}$  in Table 3) is the same as that in the dimer Dp-Cd-Cd-Dp. NBO charges on the Cd atoms and the WBI for the Cd-Cd bond is somewhat smaller than those in its Zn analogue. Again, Cd- $\text{C}_i^5$  distances suggest distorted  $\eta^5$  hapticity. Other features in the table as well as the electronic structure are similar to those in  $\text{Ep}-2\text{Zn}$ . When we turn to the process E2 of dimer formation,  $\text{Ep}-2\text{Cd}(\text{S}) + \text{Ep}-2\text{Cd}(\text{S}) \rightarrow \text{Ep}-2\text{Cd}-2\text{Cd}-\text{Ep}$ , all the data in Table 5 are related to the fact that the Cd-Cd bonds [ $E_b(\text{E2}) = -1.11 \text{ eV}$  in Table 5] is weaker than that the Zn-Zn bonds [ $E_b(\text{E2}) = -1.66 \text{ eV}$  in Table 5]. It needs to be still verified experimentally if the Cd-Ep complex can exist as dimers.

Finally, we consider the heterodimetallic complex Zn-Ep-Cd and its dimers. Table 3 shows that the binding energy of the process E1,  $\text{Zn} + \text{Ep}(\text{T}) + \text{Cd} \rightarrow \text{Zn}-\text{Ep}-\text{Cd}(\text{S})$ , is between those of the similar processes involving 2Zn and 2Cd atoms, from which all other features in the table can be explained. Note that the optimized structure adopts a syn conformation similar to that of  $\text{Ep}-2\text{Zn}$ , if we replace one of Zn atoms to a Cd atom. Table 5 also shows various parameters related to the dimerization process. Again, there are three isomers, each of them being defined in a way similar to that for Dp-2Zn-2Cd-Dp. Their binding energies  $E_b(\text{E2})$  are also between those of the corresponding processes involving 4Zn and 4Cd atoms. We again find that Zn-Cd bonds are nonpolar.

#### 4. Conclusion

Using the density functional theory within the generalized gradient approximation, we have shown variety of results on the complexes of cyclopentadienyl ligands with zinc and cadmium, starting from a landmark discovery in the chemistry of zinc.<sup>1</sup> First of all, we find that the Zn-Zn bond [ $E_b = \sim 3 \text{ eV}$ ] is stronger than bonds between transition metals, being as strong as transition metal-halide bonds. Second, the sandwich complex Cp-2Zn-Cp is shown to be physically even more stable than the complex Cp\*-2Zn-Cp\* identified by Resa et al. by 0.93 eV, which seems to correlate with release of the large space around  $\pi$  orbitals upon removal of methyl groups. Detailed analysis of electronic structures of Cp-2Zn-Cp and Cp\*-2Zn-Cp\* show that HOMO-4 represents the Zn-Zn  $\sigma$ -bond, thus explicitly confirming the existence of the covalent bond. Although less stable, similar complexes Cp- $\text{M}_1-\text{M}_2$ -Cp ( $\text{M}_1, \text{M}_2 = \text{Zn}, \text{Cd}$ ) with Cd-Cd or Zn-Cd bonds are also shown to be possible. This suggests the possible existence of the Zn-Cd covalent bond not identified thus far, requiring experimental investigation. In addition, study of dimetallic complexes of a dicyclopentadienyl ligand Dp shows that dimeric sandwich complexes of Dp-2 $\text{M}_1-2\text{M}_2$ -Dp are possible where there exist two metal-metal bonds. Similar complexes of another ligand Ep are also possible with much larger binding energy. Furthermore, the flexibility of this ligand poses the possible existence of stable monomeric complexes  $\text{M}_1-\text{Ep}-\text{M}_2$  involving only one ligand in syn conformation of two metals, which can be ascribed to the formation of a metal-metal bond facilitated by the folding of the ligand. We believe that our findings and prediction have extended our understanding on the chemistry of metal- $\pi$  interaction and metal-metal bonding involving Zn and Cd atoms, stimulating further experimental work.

Physical stability of various complexes was rigorously analyzed in terms of highly sophisticated theoretical tools, i.e.,  $l,m$ -projected electronic local density of states and electron density map for each of states around HOMO level, which clearly shows that the oxidation state of Zn is +1 as well as indicating electrostatic interaction between metal and ligands originated from the charge transfer between them. Ideal  $\eta^5$  hapticity is originated from that interaction. When there is deviation from it, it is also manifested in the electronic structures. In the sandwich complexes of the dicyclopentadienyl ligands, orientation of metal-metal bonds with respect to the ligands is shown to be dependent upon the kind of the connecting groups in the ligand, as can be easily confirmed by the comparison of Figures 3a and 9a. This would certainly affect the reactivity of the complexes and mechanism of chemical reactions involving them. Zn-Cd bond is found to be almost nonpolar, and this seems to partly reflect the symmetry of the

ligands at the two ends of Zn–Cd bond. Hence, it would be also interesting to investigate the effect of asymmetric ligands on the polarity of the bond. In addition, study on the polar Zn–M and Cd–M bonds with earlier transition metals M would be also interesting.

**Acknowledgment.** We appreciate Jeonju University for financial support.

## References and Notes

- (1) Resa, I.; Carmona, E.; Gutierrez-Puebla, E.; Monge, A. *Science* **2004**, *305*, 1136.
- (2) (a) Feng, J.; Garland, M. *Organometallics* **1999**, *18*, 417. (b) Castiglioni, M.; Deabate, S.; Giordano, R.; King, P. J.; Knox, S. A. R.; Sappa, E. *J. Organomet. Chem.* **1998**, *571*, 251. (c) Bazhenova, T. A.; Bazhenova, M. A.; Mironova, S. A.; Petrova, G. N.; Shilova, A. K.; Shuvalova, N. I.; Shilov, A. E. *Inorg. Chem. Acta* **1998**, *270*, 221. (d) Salo, E. V.; Guan, Z. *Organometallics* **2003**, *22*, 5033.
- (3) Wright, M. E.; Topikar, E. G. *Macromolecules* **1992**, *25*, 6050.
- (4) Wilbert, G.; Trand, S.; Zentel, R. *Macromol. Chem. Phys.* **1997**, *198*, 3769.
- (5) Kim, C.; Park, E.; Song, C. K.; Koo, B. W. *Synth. Met.* **2001**, *123*, 493.
- (6) Faggiani, R.; Gillespie, R. J.; Vekris, J. E. *J. Chem. Soc. Chem. Commun.* **1986**, 517.
- (7) (a) Iijima, S.; Motoyama, I.; Santo, H. *Chem. Lett.* **1979**, 1349. (b) Marinquez, J. M.; Ward, M. D.; Reiff, W. M.; Calabrese, J. C.; Jones, N. L.; Carroll, P. J.; Bunel, E. E.; Miller, J. S. *J. Am. Chem. Soc.* **1995**, *117*, 6182.
- (8) Bonifaci, C.; Cecon, A.; Gambaro, A.; Manoli, F.; Mantovani, L.; Ganis, P.; Santi, S.; Venzo, A. *J. Organomet. Chem.* **1998**, *577*, 97.
- (9) Kohler, F. H.; Schell, A.; Weber, B. *Chem.—Eur. J.* **2002**, *8*, 5219.
- (10) Kresse, G.; Hafner, J. *Phys. Rev. B* **1993**, *47*, RC558.
- (11) Kresse, G.; Furthmuller, J. *Phys. Rev. B* **1996**, *54*, 11169.
- (12) Kresse, G.; Joubert, D. *Phys. Rev. B* **1999**, *59*, 1758.
- (13) Perdew, J. P.; Burke, K.; Ernzerhof, M. *Phys. Rev. Lett.* **1996**, *77*, 3865.
- (14) Kang, H. S. *J. Phys. Chem. A* **2005**, *109*, 478.
- (15) Huheey, J. E.; Keiter, E. A.; Keiter, R. L. *Inorganic Chemistry*; Harper Collins College Publishers: New York, 1993; p A-31.
- (16) Frisch, M. J.; Trucks, G. W.; Schlegel, H. B.; Scuseria, G. E.; Robb, M. A.; Cheeseman, J. R.; Montgomery, J. A., Jr.; Vreven, T.; Kudin, K. N.; Burant, J. C.; Millam, J. M.; Iyengar, S. S.; Tomasi, J.; Barone, V.; Mennucci, B.; Cossi, M.; Scalmani, G.; Rega, N.; Petersson, G. A.; Nakatsuji, H.; Hada, M.; Ehara, M.; Toyota, K.; Fukuda, R.; Hasegawa, J.; Ishida, M.; Nakajima, T.; Honda, Y.; Kitao, O.; Nakai, H.; Klene, M.; Li, X.; Knox, J. E.; Hratchian, H. P.; Cross, J. B.; Adamo, C.; Jaramillo, J.; Gomperts, R.; Stratmann, R. E.; Yazyev, O.; Austin, A. J.; Cammi, R.; Pomelli, C.; Ochterski, J. W.; Ayala, P. Y.; Morokuma, K.; Voth, G. A.; Salvador, P.; Dannenberg, J. J.; Zakrzewski, V. G.; Dapprich, S.; Daniels, A. D.; Strain, M. C.; Farkas, O.; Malick, D. K.; Rabuck, A. D.; Raghavachari, K.; Foresman, J. B.; Ortiz, J. V.; Cui, Q.; Baboul, A. G.; Clifford, S.; Cioslowski, J.; Stefanov, B. B.; Liu, G.; Liashenko, A.; Piskorz, P.; Komaromi, I.; Martin, R. L.; Fox, D. J.; Keith, T.; Al-Laham, M. A.; Peng, C. Y.; Nanayakkara, A.; Challacombe, M.; Gill, P. M. W.; Johnson, B.; Chen, W.; Wong, M. W.; Gonzalez, C.; Pople, J. A. *Gaussian 03*, revision B.05. Gaussian, Inc.: Pittsburgh, PA, 2003.
- (17) Wiberg, K. B. *Tetrahedron* **1968**, *24*, 1083.
- (18) Reed, A. E.; Curtiss, L. E.; Weinhold, F. *Chem. Rev.* **1988**, *88*, 899.
- (19) A minor difference is that the antibonding interaction between two  $4s(\text{Zn})$  orbitals now becomes LUMO+3, not LUMO, the energy difference between them being only 0.21 eV.
- (20) Atzkern, H.; Hiermeier, J.; Kanellakopoulos, B.; Kohler, F. H.; Muller, G.; Steigelmann, O. *J. Chem. Soc., Chem. Commun.* **1991**, 997.
- (21) HOMO-2 and HOMO-1 represent mostly (HOMO-2) and (HOMO-1) of  $\text{Dp}^{2-}$ . HOMO consists of (HOMO) of  $\text{Dp}^{2-}$  and weak contribution from the bonding interaction between  $\pi(\text{C}_2^5)$  and  $s(\text{Zn})$ . This  $\text{C}_2^5\text{—Zn}$  bonding interaction corresponds to a partial bond between Zn and  $\text{C}_2^5$  atoms in Table 3 as well as that between their equivalents in other five-membered rings.
- (22)  $\text{C}_2^5$  is especially close ( $=2.06 \text{ \AA}$ ) to one of the Zn atoms, and its NBO charge ( $=-0.65$ ) is largely negative. In addition, C–C bonds ( $l = 1.46$  and  $1.46 \text{ \AA}$ ) involving that atom are longer than those ( $l = 1.41$  and  $1.43 \text{ \AA}$ ) in an isolated neutral Cp ring by at least  $0.3 \text{ \AA}$ . Three atoms,  $\text{C}_2^5\text{—Zn1—Zn2}$ , are nearly linear. WBI of the Zn–Zn bonds ( $=0.72$ ) and NBO charge ( $=0.77$ ) of Zn atoms are slightly smaller than those in Cp–Zn–Zn–Cp shown in Table 2.
- (23) LUMO+1 is characterized by the antibonding interaction of  $4s(\text{Zn})$  states, again confirming the transfer of eight electrons from the states.
- (24) Distances between Cd and carbon atoms in the five-membered rings ( $=\text{Cd—C}_i^5$ ) are at least 48% longer than those in Cp–Cd–Cd–Cp shown in Table 2. In addition, there is practically no change in  $l(\text{C}_i^5\text{—C}_{i+1}^5)$  from those of neutral Dp ring upon addition of two Cd atoms.
- (25) One minor thing we might pay attention to is the difference in the NBO charges on two kinds of metallic atoms for the isomer 3. Its electronic structure is found to be almost the same as that for the isomer 1.
- (26) Table 3 also shows that  $\text{C}_i\text{—C}_{i+1}$  distances are close to those ( $=1.43 \text{ \AA}$ ) in an isolated dianion  $\text{Ep}^{2-}$ .
- (27) In HOMO-3 and HOMO, there is weak contribution from a  $\sigma$  bond [ $=\sigma(\text{C}_1^5\text{—Zn})$ ] between  $\text{C}_1^5$  and a Zn atom nearby, in HOMO-2, from  $\sigma(\text{C}_2^5\text{—Zn})$ ,  $\sigma(\text{C}_3^5\text{—Zn})$ ,  $\sigma(\text{C}_4^5\text{—Zn})$ , and  $\sigma(\text{C}_5^5\text{—Zn})$ , suggesting distorted  $\eta^5$  hapticity.